

Subcellular Golgi localization of Stathmin family proteins is promoted by a specific set of DHHC palmitoyl transferases

Aurore D. Levy^{*,†,‡}, Véronique Devignot^{*,†,‡}, Yuko Fukata[§], Masaki Fukata[§],
André Sobel^{*,†,‡} and Stéphanie Chauvin^{*,†,‡}

Supplementary Figure legends

Figure S1. Stathmin 3 palmitoylation requires functional Golgi membranes. The level of stathmin 3 palmitoylation in 6-DIV cortical neurons in culture, treated or not (Control) with 2-BP or BFA was evaluated using the ABE (acyl-biotinyl exchange) assay (see methods). T: total N-ethyl-maleimide (NEM) quenched cell extract (1/20 volume); as a control, HAM (hydroxylamine) cleavage of palmitates was replaced by an inactive amine, Tris. Stathmin 3 was revealed on western blots with specific antibodies. Stathmin 3 appeared as several bands (HAM, ABE line). As for stathmin 2 (Figure 1B), treatment with 2-BP or BFA reduced by more than one half the level of stathmin 3 palmitoylation. Results are representative of two separate experiments that gave similar results.

Figure S2. Dispersion of the Golgi pool of stathmin 3 after 2-BP or BFA treatments. Hippocampal neurons at 6-DIV were stained for stathmin 3 (St3, green) and for either the Golgi complex (CTR433, red) or the ER (KDEL, red). For each double labeling, a single layer confocal image is shown. (A) In untreated neurons (control), stathmin 3 labeling is present at the Golgi (colocalization with CTR433) and along neurites as vesicle-like structures. 2-BP or BFA treatment resulted in the disruption of the Golgi pool of stathmin 3, whereas the vesicle-like localization was partially abolished. Higher magnification of the boxed neurite and soma regions in merged images better illustrates the dispersion of the Golgi stathmin 3 labeling as well as the small size of the remaining vesicle-like structures after both treatments. (B) Following BFA treatment, stathmin 3 labeling did not merge perfectly with that of the ER (KDEL), neither in the soma nor within neurites (see higher magnification of the merged images). (C) The subcellular localization of stathmin 3 was analyzed after cell fractionation

that separates the soluble (S) and membrane (M) fractions from total extracts (T) of untreated (C), 2-BP or BFA treated hippocampal neurons. Equivalent volumes of each fraction were analyzed by SDS-PAGE and Western blotted for stathmin 3. (D) Quantification of the membrane and soluble pools of stathmin 3 expressed as a percentile of stathmin 3 in the total extract. Whereas stathmin 3 was present in majority in the membrane fraction in the control, it was significantly redistributed from the membrane to the soluble fraction after 2-BP or BFA treatment. Values are mean \pm SEM (n=3). The statistical significance of differences between the percentage of stathmin 3 in membrane fractions when treated or not by 2-BP or BFA was assessed by a Student's t test. *, $p < 0.05$.

Figure S3. A specific set of DHHC PATs partially colocalized with stathmin 3 at the Golgi complex in hippocampal neurons. Hippocampal neurons transfected at 6-DIV with the indicated myc- or HA-tagged DHHCs were immunostained for endogenous stathmin 3 (St3, green), and either HA- or myc- to visualize exogenous DHHCs (red), and CTR433 to visualize the Golgi complex (blue). (A) As for stathmin 2 (Figures 3 and 4A), DHHC3, -7, and -17 displayed a full colocalization with CTR433, and an extensive colocalization at the Golgi with endogenous stathmin 3, also present along neurites as a vesicle-like labeling. (B) Similarly to stathmin 2 (Figure 4B), DHHC9, -12 and -15 colocalized with endogenous stathmin 3 at the Golgi (colocalization with CTR433 in Figure S4) and labeled neurites as vesicle-like structures not overlapping with those labeled for stathmin 3. DHHC22 colocalized as well with endogenous stathmin 3 at the Golgi, but also showed an extra-Golgi ER labeling (Figure S4). DHHC4 did not fully colocalize with stathmin 3 at the Golgi but mainly localized to the ER (Figure S4). Bars=10 μ M; boxed areas in the merged images are shown at higher magnification.

Figure S4. Golgi-localized DHHCs are either restricted or also present at the ER in hippocampal neurons. Hippocampal neurons transfected at 6-DIV with myc- or HA-tagged DHHC4, -9, -12, -15 and 22 were labeled for exogenous DHHCs (green), and either (A) a Golgi (CTR433, red) or (B) an ER marker (KDEL, red). Subcellular localization of DHHCs were examined by confocal microscopy, with boxed areas in the merged images shown at higher magnification. DHHC12 and -15 displayed an extensive colocalization with CTR433

at the Golgi (A), and some additional labeling at vesicles in neurites, but no overlapping with the ER as shown with KDEL for DHHC12 (B). DHHC9 and -22 were both localized at the Golgi and the ER, as shown by partial colocalization with both CTR433 (A) and KDEL (B). DHHC4 was localized mainly at the ER as illustrated by an extensive colocalization with KDEL (B). Bars=10 μ M.

Figure S5. DHHC3, -7, -15 and -17 specifically interact with the A targeting domain of stathmin 3. The N-terminal targeting domain of stathmin 3 fused to GFP (A3-GFP) was cotransfected in HeLa cells with either (A) myc-tagged DHHCs or (B) HA-tagged DHHC3, and the corresponding cell lysates were tested for coimmunoprecipitation with A3-GFP using either anti-myc or anti-HA antibodies. (A) Immunoprecipitation of myc-tagged DHHCs revealed an interaction of DHHC3, -7, -15 and -17 with A3-GFP. Cells with A3-GFP and the empty vector used for DHHC expression were processed as a control (lane 1). (B) Interaction between A3-GFP and DHHC3 was revealed after immunoprecipitation of both HA-tagged DHHC3 or A3-GFP. Anti-GFP antibody precipitated two major forms of A3-GFP whereas anti-HA coimmunoprecipitated mainly the lower one (arrowhead). Note the presence of an IgG band revealed in the top panel corresponding to the immunoprecipitation of HA-DHHC3. These data are representative of three independent experiments that gave similar results.

Figure S6. Stathmin 3 membrane binding is regulated by DHHC3, -7, -15 and -21. Individual HA-tagged DHHCs were cotransfected in HeLa cells with stathmin 3 (St3) (WT or palmitoylation deficient mutant C22A/C24A) and fractionated into soluble (S) and membrane (M) fractions. Aliquots of the total extract (T) and equal volumes of the recovered S and M fractions were analyzed by western blot using anti-myc antibody for stathmin 3, and anti-HA (for DHHC3, -7, -15 and -21) or anti-myc (for DHHC22) antibodies for DHHCs. In the total extract (T), stathmin 3 migrated (arrows) as an upper double band and a lower cleaved one. (A) When stathmin 3 was transfected alone, the uncleaved forms were accumulated in both the soluble and membrane fraction (majority in the membrane fraction), whereas its palmitoylation deficient mutant C22A/C24A was enriched in the soluble fraction, in the presence or not of DHHC3. Inactive DHHC3 (C/S) had not effect on the repartition of stathmin 3. Wild type DHHC3, as well as (B) DHHC7 and -15 specifically and significantly

enhanced the enrichment of stathmin 3 in the membrane fraction. In spite of a weak level of expression, DHHC21 was able to enhance significantly stathmin 3 membrane binding. The "non-specific" DHHC22 was hardly efficient. Note that, as for stathmin 2 (Figure 7), overexpression of all DHHCs induced an increase in the level of stathmin 3 expression. (C) Quantification of the membrane and the soluble pool of stathmin 3 transfected together with each of the DHHC proteins. The intensity of the upper forms of stathmin 3 in each fraction was quantified in comparison with their intensity in the total extract (T). Values are the mean of two independent experiments (except for DHHC3 C/S). Each horizontal bar corresponds to one value from one experiment.

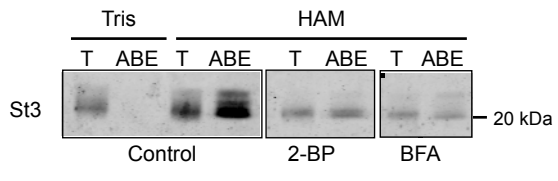


Fig. S1

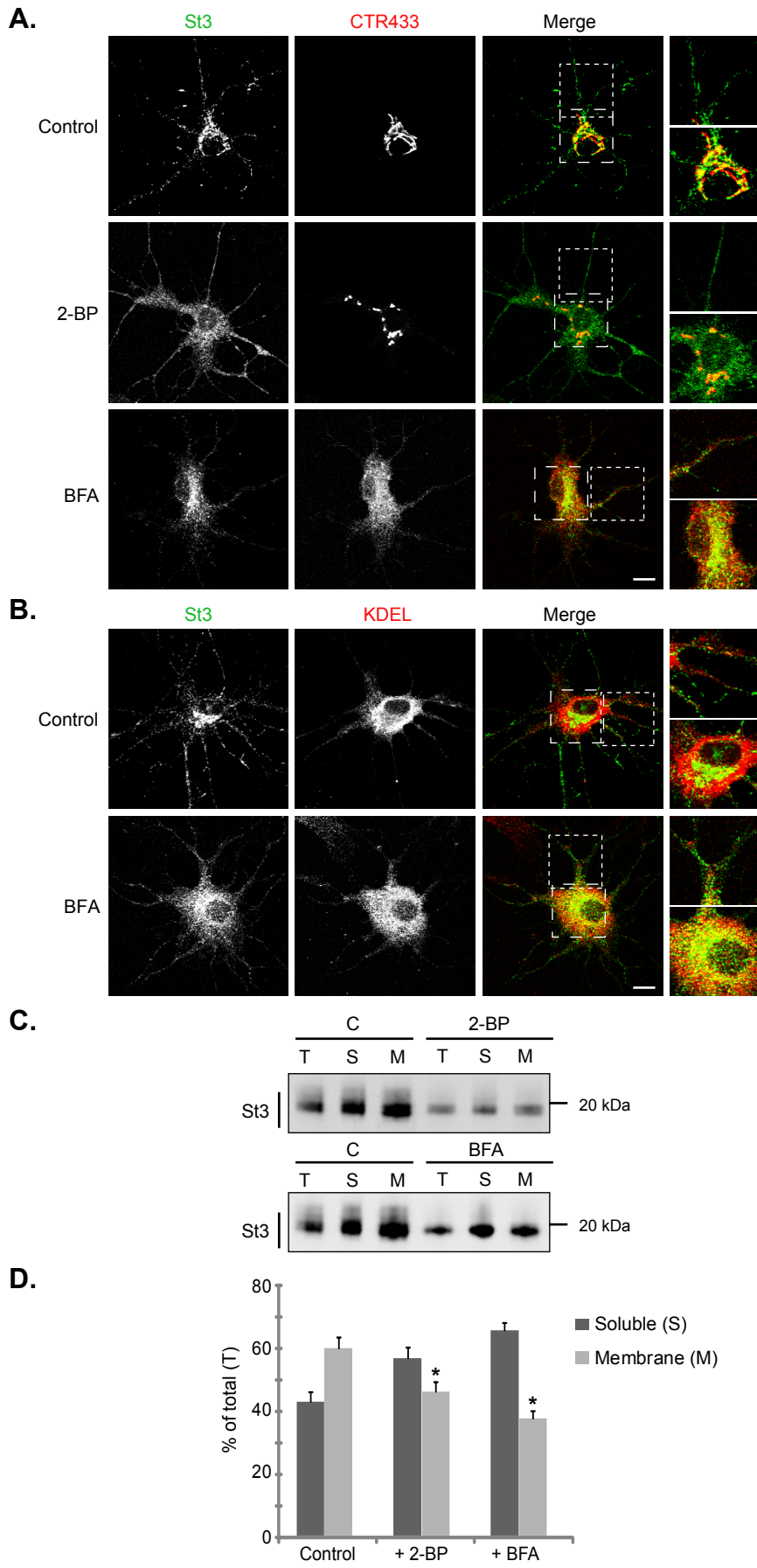


Fig. S2

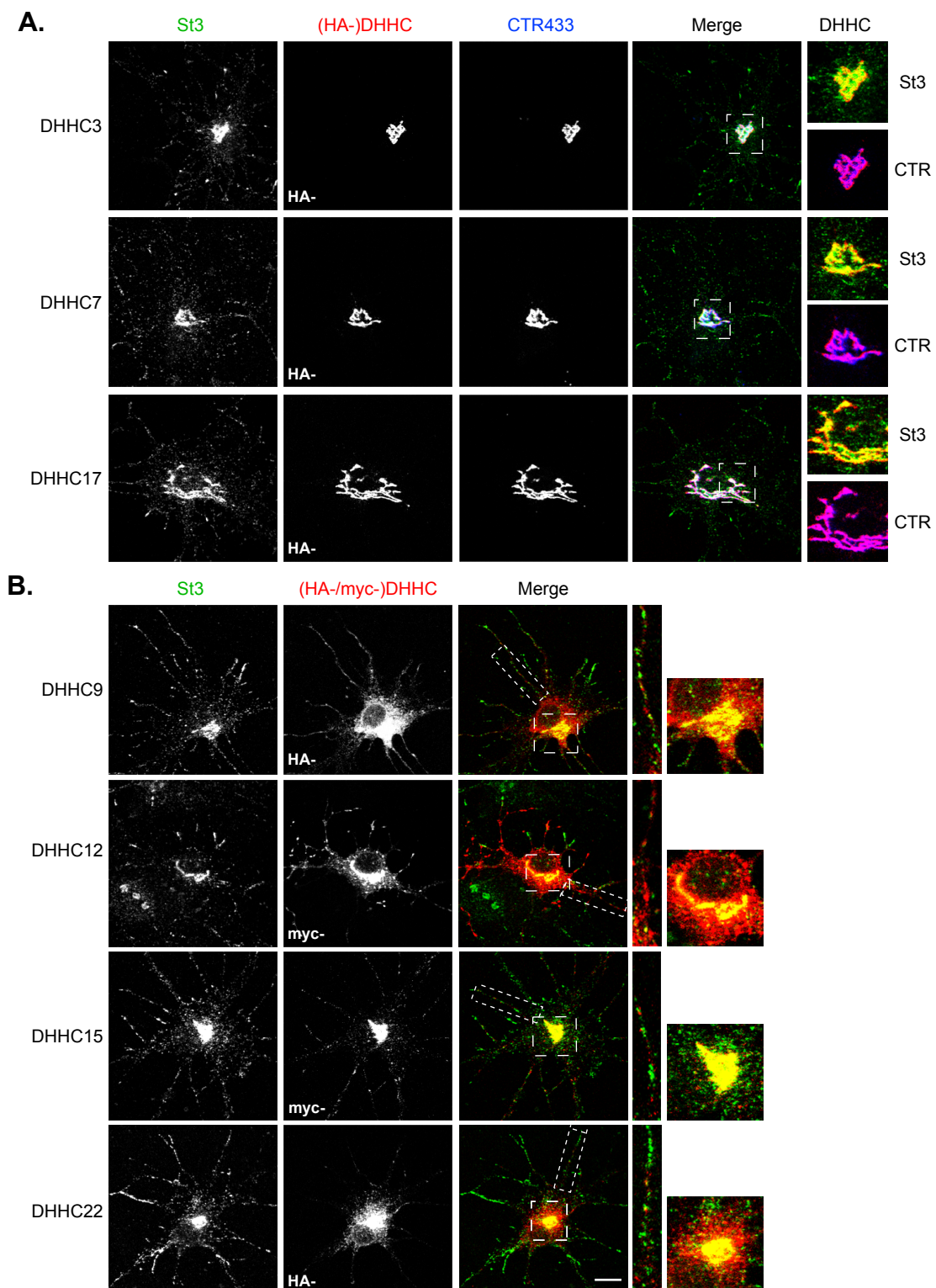


Fig. S3

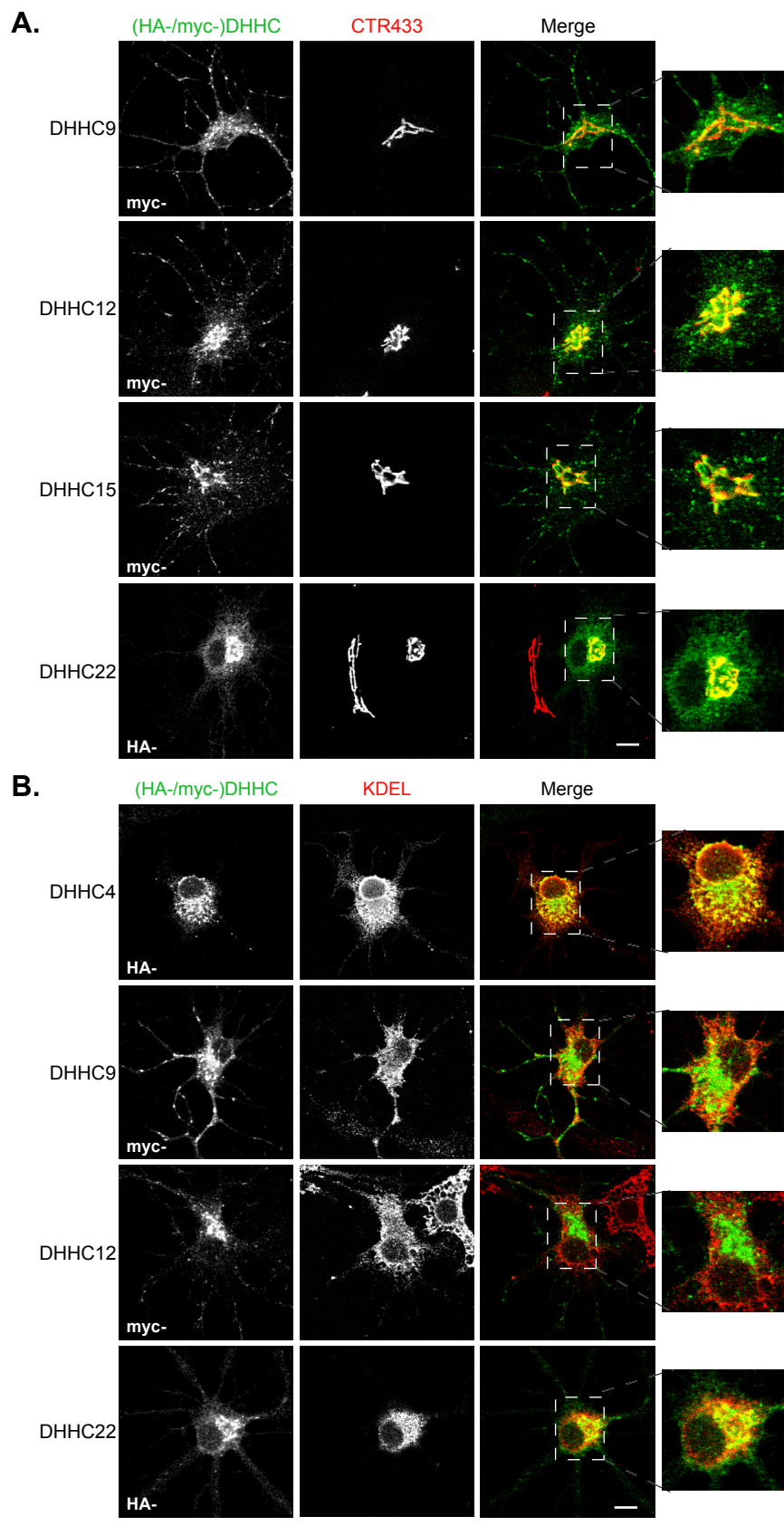


Fig. S4

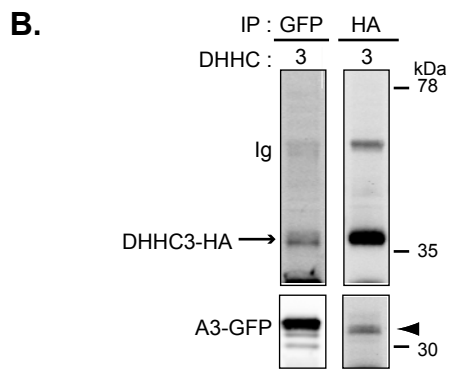
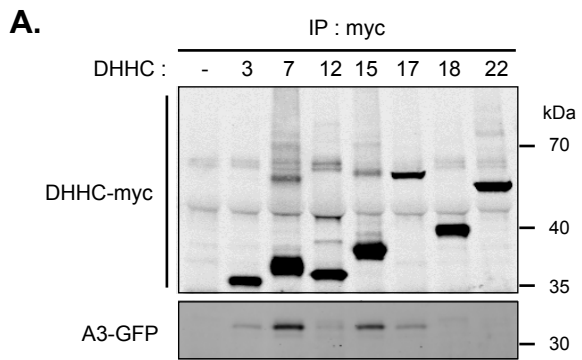


Fig. S5

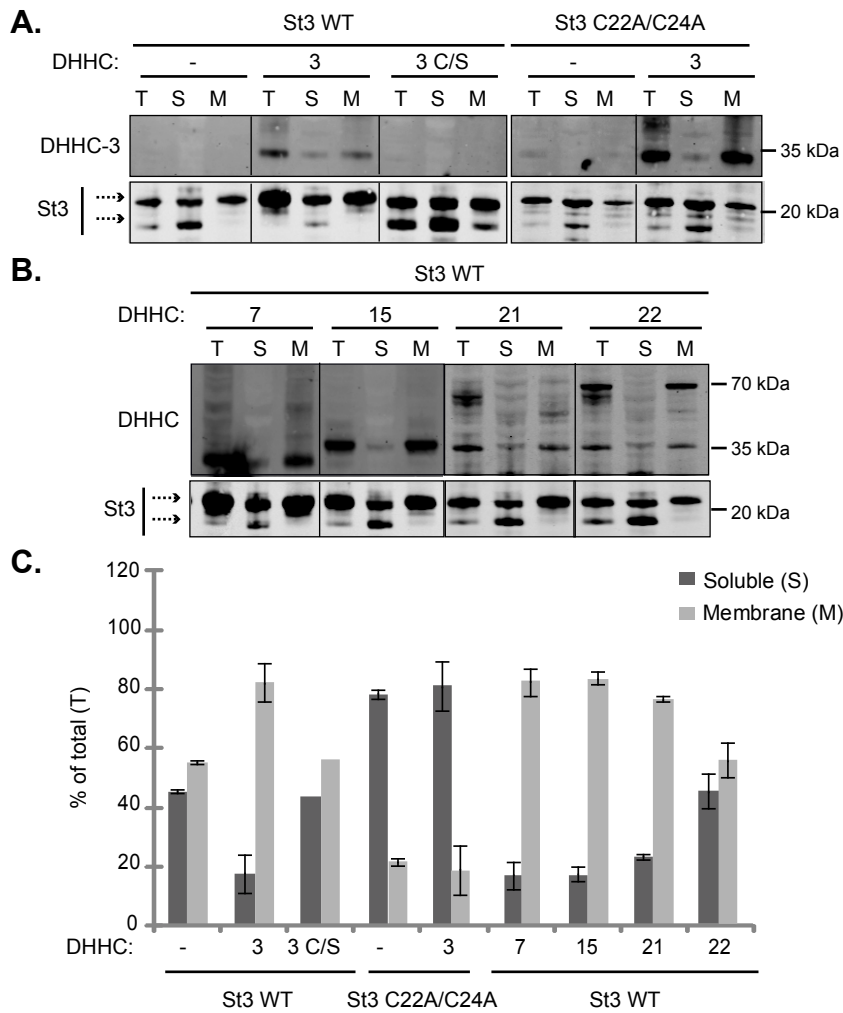


Fig. S6